



OPEN ACCESS

ORIGINAL RESEARCH

# Latest generation of flat detector CT as a peri-interventional diagnostic tool: a comparative study with multidetector CT

Johanna Rosemarie Leyhe,<sup>1</sup> Ioannis Tsogkas,<sup>1</sup> Amélie Carolina Hesse,<sup>1</sup> Daniel Behme,<sup>1</sup> Katharina Schregel,<sup>1</sup> Ismini Papageorgiou,<sup>1</sup> Jan Liman,<sup>2</sup> Michael Knauth,<sup>1</sup> Marios-Nikos Psychogios<sup>1</sup>

► Additional material is published online only. To view please visit the journal online (<http://dx.doi.org/10.1136/neurintsurg-2016-012866>).

<sup>1</sup>Department of Neuroradiology, University Medicine Goettingen, Goettingen, Germany

<sup>2</sup>Department of Neurology, University Medicine Goettingen, Goettingen, Germany

## Correspondence to

Dr M-N Psychogios, Department of Neuroradiology, University Medicine Goettingen, Robert-Koch-Str 40, Goettingen 37075, Germany; [m.psychogios@med.uni-goettingen.de](mailto:m.psychogios@med.uni-goettingen.de)

Received 8 November 2016

Revised 28 November 2016

Accepted 29 November 2016

Published Online First

20 December 2016

## ABSTRACT

**Background and purpose** Flat detector CT (FDCT) has been used as a peri-interventional diagnostic tool in numerous studies with mixed results regarding image quality and detection of intracranial lesions. We compared the diagnostic aspects of the latest generation FDCT with standard multidetector CT (MDCT).

**Materials and methods** 102 patients were included in our retrospective study. All patients had undergone interventional procedures. FDCT was acquired peri-interventionally and compared with postinterventional MDCT regarding depiction of ventricular/subarachnoidal spaces, detection of intracranial hemorrhage, and delineation of ischemic lesions using an ordinal scale. Ischemic lesions were quantified with the Alberta Stroke Program Early CT Scale (ASPECTS) on both examinations. Two neuroradiologists with varying grades of experience and a medical student scored the anonymized images separately, blinded to the clinical history.

**Results** The two methods were of equal diagnostic value regarding evaluation of the ventricular system and the subarachnoidal spaces. Subarachnoidal, intraventricular, and parenchymal hemorrhages were detected with a sensitivity of 95%, 97%, and 100% and specificity of 97%, 100%, and 99%, respectively, using FDCT. Gray–white differentiation was feasible in the majority of FDCT scans, and ischemic lesions were detected with a sensitivity of 71% on FDCT, compared with MDCT scans. The mean difference in ASPECTS values on FDCT and MDCT was 0.5 points (95% CI 0.12 to 0.88).

**Conclusions** The latest generation of FDCT is a reliable and accurate tool for the detection of intracranial hemorrhage. Gray–white differentiation is feasible in the supratentorial region.

## INTRODUCTION

In the past decade, non-contrast flat detector CT (FDCT), acquired with angiography systems, has been used primarily for postinterventional detection of complications, such as subarachnoidal or parenchymal hemorrhage (PH).<sup>1</sup> Multiple studies comparing the diagnostic features of FDCT with multidetector CT (MDCT) have shown good image quality in the supratentorial region, with reliable detection of large hemorrhages, albeit limited image quality in the infratentorial region due to diverse image artifacts.<sup>2–4</sup> Detection of ischemic

lesions with FDCT has been inconsistent to date, due to the inferior contrast resolution and diverse artifacts of the cone beam acquisition. The latest generation of FDCT promises improved image quality.

The new high dynamic range flat detector with a 16 bit analog–digital conversion in combination with an entire image processing pipeline as well as a reconstruction algorithm chain running on 16 bit allows for enhanced soft tissue resolution. This technology package results in four times more gray value differentiation compared with conventional systems. Improved FDCT fidelity in the detection of hemorrhagic and ischemic lesions could expand the role of FDCT in acute stroke diagnostics (so called ‘one stop management’) with a possible impact on door to groin times.

In this study, we tested and compared latest generation FDCT images with standard MDCT scans regarding depiction of ventricular/subarachnoidal spaces, detection of ischemic/hemorrhagic lesions, and the presence of artifacts.

## METHODS

We retrospectively screened all angiographic procedures in our department after installation of the latest generation angiography suite (Artis Q Angiography System; Siemens Healthcare GmbH, Forchheim, Germany) from September 2014 to April 2016 for acquisition of FDCT. Patients with FDCT scans were then screened for postinterventional MDCT scans. Only patients with complete FDCT and MDCT scans were included in our analysis. Three scans with marked motion artifacts were excluded. The ethics committee of our hospital waived the need for a formal application or informed patient consent due to the retrospective design of this study.

FDCT was acquired with a biplane flat detector angiography system using the following parameters: 20 s of rotation; 200° total angle with approximately 500 projections; 2×2 binning; 109 kV; 1.8 µGy/frame; weighted CT dose index (CTDI<sub>w</sub>) ~60 mGy, effective dose ~2.5 mSv. Initial FDCT projections were then reconstructed on a postprocessing workstation (Syngo X Workplace; Siemens Healthcare GmbH) with a ‘HU smooth’ kernel and ‘DynaCT Clear’ algorithm to images with a 512×512 matrix. MDCT was acquired on a 128



CrossMark

**To cite:** Leyhe JR, Tsogkas I, Hesse AC, et al. *J NeuroIntervent Surg* 2017;**9**:1253–1257.

slice CT scanner (Somatom Definition AS+; Siemens Healthcare GmbH) using a standard brain scan protocol. Raw FDCT and MDCT data were extracted from the department's picture archiving and communication system, anonymized, reconstructed parallel to the orbitomeatal plane with a slice thickness of 5 mm and slice distance of 3 mm, and imported for evaluation into the aforementioned postprocessing workstation.

Two neuroradiologists (M-NP, >5 years of experience; IT, <5 years of experience) and a medical student (ACH), analyzed all of the images using a 3 point ordinal scale (0=not identifiable; 1=identifiable, but not diagnostic; 2=diagnostic) for the following structures/entities: supratentorial ventricular system, infratentorial ventricular system, supratentorial subarachnoidal space, infratentorial subarachnoidal space, and gray-white differentiation of the basal ganglia, insula, central region, and cerebellum. Raters were asked to identify subarachnoidal hemorrhage (SAH), intraventricular hemorrhage (IVH), PH, count the number of slices depicting blood, and measure the dimension of PH. All hemorrhages were divided into three groups with respect to the number of slices containing blood: 0–25 percentile (few), 25–75 percentile (several), and 75–100 percentile (many). In addition, raters were asked to subjectively score image quality for hemorrhage detection using a 5 point ordinal scale (very good; good; mediocre; low; bad). The presence of ischemic lesions was noted, and the Alberta Stroke Program Early CT Scale (ASPECTS) was calculated. Various types of artifacts were documented. Finally, raters were asked if they were confident about the detection/exclusion of a hemorrhage or a large ischemic lesion (ASPECTS 0–4).

Scans were divided into two random groups, consisting of FDCT and MDCT scans, and rated with a 30 day gap in between to minimize recall bias. Window levels were not predefined in order to enhance the detection of ischemic lesions. The initial reconstruction dataset (slice thickness of 0.4 mm for FDCT and 0.6 mm for MDCT) was also available and could be used at the raters' discretion. Cases of disagreement regarding detection of hemorrhage or ischemia were settled by consensus. Raters were blinded to all clinical information.

Contingency tables and the Wilcoxon test for paired samples were used to compare scores within categories. Categorical variables were compared between groups using Fischer's exact test. Receiver operating characteristic curve analysis was applied to

calculate sensitivity and specificity of FDCT for detection of hemorrhage and ischemia compared with MDCT as the gold standard. Measurements of PH as well as ASPECTS ratings on FDCT and MDCT were compared with the Bland–Altman plot. Interobserver agreement was evaluated with Spearman's coefficient of rank correlation. All tests were calculated with the MedCalc statistical package (MedCalc 16.8; MedCalc Software bvba, Ostend, Belgium). The significance level for all tests was set at  $\alpha=0.05$ .

**RESULTS**

Of the 105 patients identified, 3 were excluded due to severe motion artifacts on FDCT and hence 102 patients were included in our study (50 women; median age 63.5 years, IQR 53–77). Median time between FDCT and MDCT was 4.3 hours (IQR 1.5–6). Patients were examined after coiling, clipping, stenting, thrombectomy, and plain cerebral angiography in 24, 1, 12, 48, and 17 cases, respectively. FDCT proved to be equivalent to MDCT in the delineation of the supratentorial ventricular system and supratentorial spaces, with 102 (100%) and 98 (96%) 'diagnostic' values, respectively (table 1). Scores for the infratentorial ventricular system and infratentorial subarachnoidal spaces on FDCT were slightly worse, with 92 (90%) and 75 (74%) scans being scored as 'diagnostic' (figure 1C). However, there was no statistically significant difference in the ratings of the ventricular system or subarachnoidal spaces between FDCT and MDCT ( $p=0.106$  and  $p=0.177$ ). Gray-white differentiation was feasible on FDCT with 95%, 92%, and 96% of 'diagnostic' values in the supratentorial region and no statistically significant difference from MDCT for the basal ganglia, insular cortex, and central region (table 1).

Gray-white differentiation on FDCT was limited in the infratentorial region with significantly different scores compared with MDCT ( $p<0.001$ ). Detection of ischemic lesions was feasible on FDCT scans with 71% sensitivity and 94% specificity ( $p<0.001$ ; area under the curve (AUC) 0.83, 95% CI 0.74 to 0.89) compared with MDCT scans. Additionally, ASPECTS ratings on FDCT (figure 2C) showed a mean difference of 0.5 points (95% CI 0.12 to 0.88) in the Bland–Altman plot (see online supplementary figure S1A) compared with ratings of MDCT images. When asked about their opinion on ischemic lesion detectability, raters stated that in 98% and 99% of cases

**Table 1** Rating of cerebral structures

Variable		Diagnostic n (%)	Identifiable but not diagnostic n (%)	Not identifiable n (%)	Total n (%)	Wilcoxon p Value
Supratentorial ventricular system	FDCT	102 (100)	0 (0)	0 (0.0)	102 (100)	–
	MDCT	102 (100)	0 (0)	0 (0.0)	102 (100)	
Infratentorial ventricular system	FDCT	92 (90)	9 (9)	1 (1)	102 (100)	0.106
	MDCT	98 (96)	3 (3)	1 (1)	102 (100)	
Supratentorial subarachnoidal space	FDCT	98 (96)	4 (4)	0 (0)	102 (100)	0.813
	MDCT	99 (97)	3 (3)	0 (0)	102 (100)	
Infratentorial subarachnoidal space	FDCT	75 (74)	25 (25)	2 (2)	102 (100)	0.177
	MDCT	85 (83)	14 (14)	3 (3)	102 (100)	
Gray-white differentiation of basal ganglia	FDCT	97 (95)	5 (5)	0 (0)	102 (100)	0.563
	MDCT	99 (97)	3 (3)	0 (0)	102 (100)	
Gray-white differentiation of insular cortex	FDCT	94 (92)	8 (8)	0 (0)	102 (100)	0.625
	MDCT	96 (94)	6 (6)	0 (0)	102 (100)	
Gray-white differentiation of central cortex	FDCT	98 (96)	4 (4)	0 (0)	102 (100)	0.813
	MDCT	99 (97)	3 (3)	0 (0)	102 (100)	
Gray-white differentiation of cerebellum	FDCT	57 (56)	37 (36)	8 (8)	102 (100)	<0.001
	MDCT	88 (86)	13 (13)	1 (1)	102 (100)	

FDCT, flat detector CT; MDCT, multidetector CT.

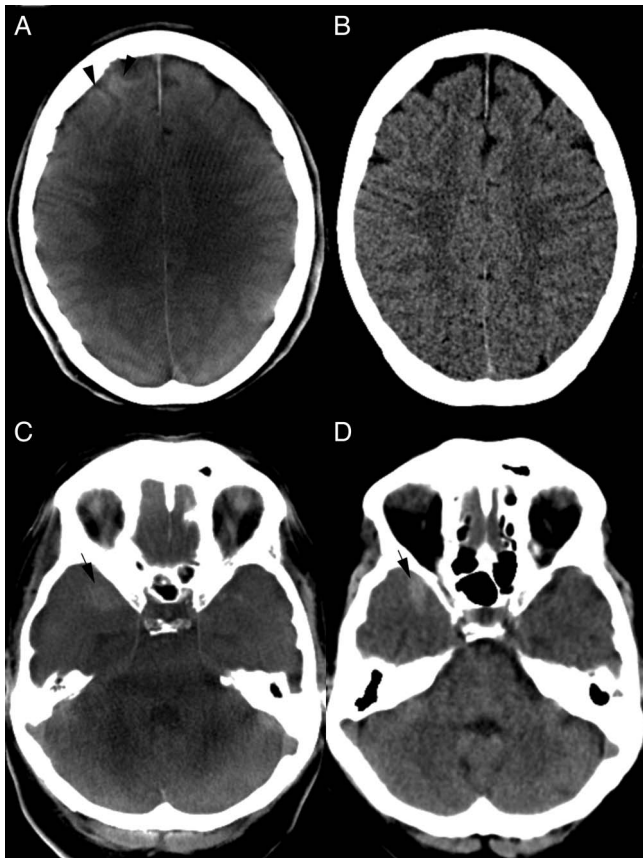


**Figure 1** (A, B) CT images after balloon assisted coil embolization of an anterior communicating artery aneurysm. (A) Flat detector CT (FDCT) shows a cortical hyperattenuation of the right frontal lobe (black arrowhead). A subarachnoid hemorrhage (SAH) can be excluded on both FDCT (A) and follow-up multidetector CT (MDCT) (B) images. Gray–white matter differentiation as well as exclusion of postinterventional ischemic lesions is feasible in both examinations. (C, D) Right temporal SAH. Blood is delineated on both FDCT (C) and MDCT (D) examinations (black arrows). Gray–white matter differentiation of the cerebellum is limited on FDCT (C) but the fourth ventricle is clearly depicted and an intraventricular hemorrhage can be excluded.

they were sure about the detection/exclusion of extended (ASPECTS <5) ischemic lesions on FDCT and MDCT, respectively ( $p=0.019$ ).

SAH was diagnosed in 39 cases with FDCT; 37 were true positives, resulting in a sensitivity of 95% and a specificity of 97% (see online supplementary table S1;  $p<0.001$ ; AUC 0.96, 95% CI 0.89 to 0.98) (figure 3). One false negative FDCT scan included an SAH seen on a few slices (group with 2–12) on MDCT and one seen on several MDCT slices (group with 12–33). Thirty-three of the 34 IVH cases were detected on FDCT ( $p<0.001$ ; AUC 0.98; 95% CI 0.93 to 0.99). The one false negative FDCT scan included an IVH seen on a few slices (group with 2–4) on MDCT. All cases diagnosed with PH on MDCT were also depicted and scored similarly on FDCT, resulting in 100% sensitivity and 99% specificity of FDCT for the detection of PH ( $p<0.001$ ; AUC 0.99; 95% CI 0.95 to 1.00). The median slice count of PH on MDCT was 10 (IQR 8–13). The mean difference between PH measurements on FDCT and MDCT was  $-35.13 \text{ mm}^2$  (95% CI  $-88.67$  to  $18.39 \text{ mm}^2$ , see online supplementary figure S1B). In the supratentorial region, raters found ‘very good’ image quality for hemorrhage detection in 87% of FDCT scans compared with 93% of MDCT

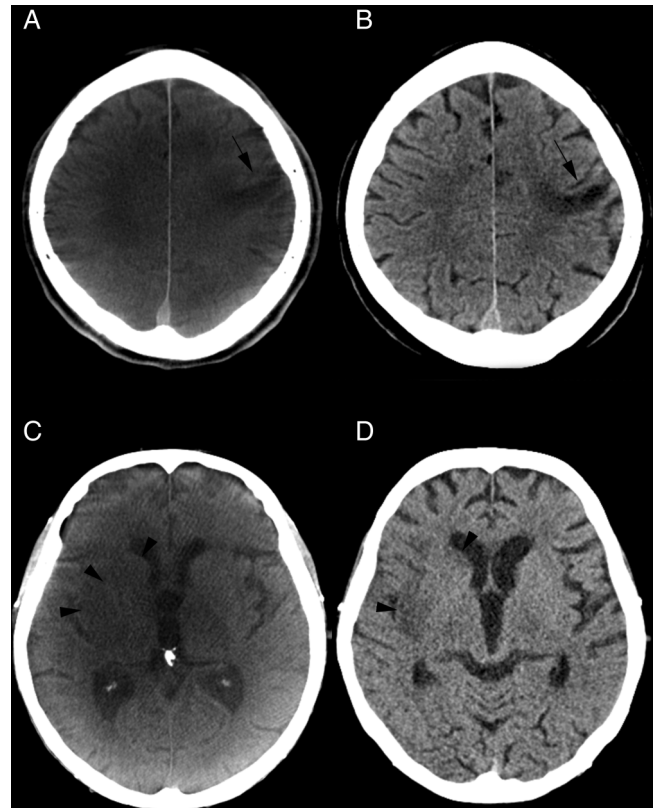


**Figure 2** (A) An older small cortical infarction is depicted on the flat detector CT (FDCT) scan after carotid artery stenting (A, black arrow). No acute ischemic lesions were detected on this scan. The same lesion can be confirmed on multidetector CT (MDCT) (B, black arrow). (C, D) CT images prior to thrombectomy and at follow-up. Acute ischemic lesions can be seen on non-contrast FDCT (C, black arrowheads) performed prior to thrombectomy. An intracranial hemorrhage can be excluded and an Alberta Stroke Program early CT Scale (ASPECTS) score of 7 can be rated on FDCT images. Ischemic lesions are confirmed on follow-up MDCT images (D, black arrowheads) after rapid reperfusion.

examinations ( $p=0.266$ ). A statistically significant difference was shown in the same category of scores in the infratentorial region, with 58% of ‘very good’ scores on FDCT compared with 78% on MDCT ( $p=0.002$ ). When asked about their subjective judgement on hemorrhagic lesion detectability, raters stated that in 98% and 99% of cases they were sure about the detection/exclusion of hemorrhagic lesions on FDCT and MDCT, respectively ( $p=1$ ).

Metal artifacts were delineated in 22% of FDCT scans, with only one case with significant degradation of image quality. Motion, ring, and burn-in artifacts were visible on 26%, 23%, and 24% of FDCT scans, respectively. Streak artifacts were present on the majority of FDCT scans (72%). However, most artifacts only slightly affected the image quality of FDCT scans.

The highest correlation coefficient between overall raters’ scores was documented between the two physicians ( $r=0.80$ ; 95% CI 0.79 to 0.81) while lower values were documented between the experienced physician and the medical student ( $r=0.71$ ; 95% CI 0.69 to 0.73) as well as the inexperienced physician and the medical student ( $r=0.69$ ; 95% CI 0.68 to 0.71).

## DISCUSSION

The primary use of FDCT to date has been limited to detection of peri-interventional complications, such as SAH after coiling

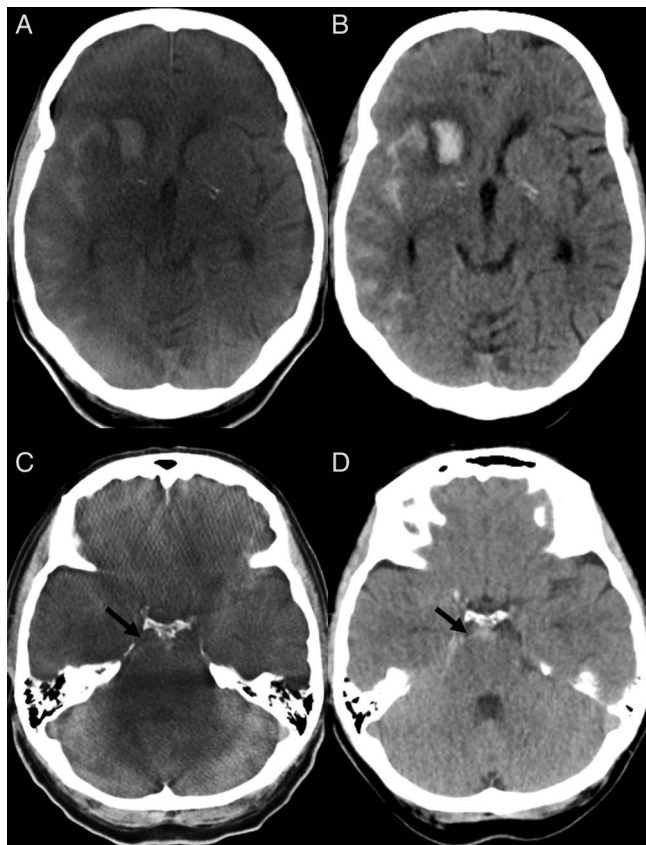


**Figure 3** A parenchymal hemorrhage and subarachnoid hemorrhage (SAH) can be diagnosed on flat detector CT (FDCT) (A) and verified on follow-up multidetector CT (MDCT) (B). (C, D) A small SAH can be seen in the preponine cistern on FDCT (C, black arrow) images. The same findings were delineated on follow-up MDCT (D, black arrow).

of an intracranial aneurysm or PH after thrombectomy of a large vessel occlusion. Multiple studies have documented the limitations of previous generations of FDCT in the detection of intracranial hemorrhages and ischemic lesions.<sup>2–4</sup> Such limitations have restricted the use of FDCT as a primary imaging modality in acute stroke imaging because administration of intravenous recombinant tissue plasminogen activator as the gold standard stroke therapy up to 2015 required reliable exclusion of hemorrhage prior to therapy initiation. In the new era of acute stroke treatment, reliable differentiation between ischemic and hemorrhagic stroke remains a fundamental element of multimodal stroke imaging. Depiction of early ischemic signs has lost importance within the first 6 hours after symptom onset, as even patients with extended ischemic lesions (ASPECTS 0–5) may profit from thrombectomy.<sup>5,6</sup>

We found FDCT to be as reliable and accurate as MDCT in the detection of intracranial hemorrhage. High sensitivity and specificity was shown for SAH and IVH. Two of the false negative cases were associated with extensive motion artifacts on FDCT and were visible on only a few MDCT slices. All PH, regardless of size or intracranial location, were depicted and diagnosed on FDCT. Gray–white differentiation in the supratentorial region was feasible with the latest generation of FDCT, as there was no statistically significant difference in scores compared with MDCT. Moreover, detection of ischemic lesions was much improved compared with previous generations of FDCT,

as we found 71% sensitivity compared with the gold standard MDCT.<sup>4</sup>

The new generation of FDCT promises much better gray–white differentiation due to the high dynamic range flat detector, enabling four times more gray value differentiation, approaching the contrast resolution of conventional MDCT. Artifacts near the skull base are reduced due to new reconstruction algorithms.<sup>7</sup> Furthermore, the latest generation of X-ray tubes enables higher maximum tube current than earlier systems, which reduces voltage variation and enables better penetration during the acquisition, especially in larger sized patients. In addition, it provides a full set of quadratic and generally smaller focal spot sizes, thus enhancing image sharpness in all viewing directions. As in previous studies, delineation of supratentorial ventricles was excellent with FDCT. Compared with past generations of FDCT, a significant improvement was observed in the infratentorial region, as we found 74% and 90% of FDCT scans to be of ‘diagnostic’ quality regarding depiction of subarachnoid spaces and of the fourth ventricle, respectively (29% and 61% in a previous study).<sup>4</sup> However, with limited diagnostic quality in 26% of FDCT scans, detection of small infratentorial SAH can be challenging. This fact should be taken into consideration in future studies evaluating the use of FDCT as a primary triage tool in stroke. The radiation dose of the FDCT scan used in our study is comparable with incremental MDCT examinations with an effective dose of approximately 2.5 mSv.<sup>8,9</sup>

The primary limitation of our study is its retrospective character. As FDCT and MDCT scans were acquired with a time delay, we cannot exclude false negative results due to new hemorrhage or demarcation of ischemic lesions. Two false positive SAH cases on FDCT were a result of contrast media extravasation after a long intervention which was falsely rated as an SAH on FDCT but resolved after a few hours on MDCT. Lastly, FDCT detectability of ischemic lesions and gray–white differentiation may have been enhanced by the presence of contrast media, in cases where FDCT was performed postinterventionally.

Our results may impact the management of acute stroke patients. After publication of the ‘unhappy triad’ of negative trials in 2013, time from hospital admission to reperfusion was identified as a reason for the negative results, in addition to the use of older devices and low reperfusion rates.<sup>10–12</sup> The authors of the ‘unhappy triad’ trials reported significant delays to initiation of endovascular treatment, with up to 120 min from imaging to groin puncture. In-hospital times were much improved in the five positive randomized trials published in 2015, with a median door to groin time of 104 min. However, only 13% and 4% of the randomized patients were treated within the ‘ideal’ SNIS 2015 intervals of  $\leq 60$  min for door to groin time and  $\leq 30$  min for imaging to groin time.<sup>13</sup> Even with a streamlined process, Frei *et al*<sup>14</sup> recently reported a median door to groin time of 71 min for direct admission patients undergoing triage with MDCT.

Implementation of a one stop management for stroke patients could lead to a reduction in in-hospital times. In our department, we estimated a time gain of approximately 30 min if we bypass MDCT and transport patients with suspected large vessel occlusions directly to the angio suite (Psychogios MN, unpublished data, 51th Meeting of the German Society of Neuroradiology, [http://dgnr.conference2web.com/content/748/details?from\\_view=all](http://dgnr.conference2web.com/content/748/details?from_view=all), 2016). The addition of flat detector CT perfusion or multiphase flat detector CT angiography allows the acquisition of multimodal CT within the angio suite as a complete stroke

imaging battery without relevant limitations compared with MDCT multimodal imaging.<sup>15 16</sup>

## CONCLUSIONS

The latest generation of FDCT is a reliable and accurate tool for the detection of intracranial hemorrhage. Gray–white differentiation is feasible in the supratentorial region but seems limited for the infratentorial brain.

**Contributors** Guarantor of the integrity of the entire study: M-NP. Study concepts: MK and M-NP. Study design: M-NP, JRL, IT, and ACH. Definition of intellectual content: M-NP, IT, and JRL. Literature research: M-NP, JRL, DB, and KS. Clinical studies: IT, JRL, DB, KS, and ACH. Data acquisition: IT, JRL, DB, and KS. Data analysis: M-NP, MK, IP, and ACH. Statistical analysis: M-NP, JRL, and IP. Manuscript preparation: M-NP, JL, and JRL. Manuscript editing: M-NP and DB. Manuscript review: M-NP, MK, JL, and IP.

**Competing interests** The Department of Neuroradiology, University Medicine Goettingen, has a research agreement with Siemens Healthcare GmbH, Forchheim, Germany.

**Ethics approval** The study was approved by the ethics committee of University Medicine Goettingen. The ethics committee of our hospital waived the need for a formal application or informed patient consent due to the retrospective design of this study.

**Provenance and peer review** Not commissioned; externally peer reviewed.

## Previous or future presentations

DGNER, October 2016, German Neuroradiology Society Meeting, Cologne, Germany; International Stroke Conference, February 2017, Houston, Texas, USA.

**Open Access** This is an Open Access article distributed in accordance with the Creative Commons Attribution Non Commercial (CC BY-NC 4.0) license, which permits others to distribute, remix, adapt, build upon this work non-commercially, and license their derivative works on different terms, provided the original work is properly cited and the use is non-commercial. See: <http://creativecommons.org/licenses/by-nc/4.0/>

## REFERENCES

- Heran NS, Song JK, Namba K, et al. The utility of DynaCT in neuroendovascular procedures. *AJNR Am J Neuroradiol* 2006;27:330–2.
- Söderman M, Babic D, Holmin S, et al. Brain imaging with a flat detector C-arm: technique and clinical interest of XperCT. *Neuroradiology* 2008;50:863–8
- Struffert T, Richter G, Engelhorn T, et al. Visualisation of intracerebral haemorrhage with flat-detector CT compared to multislice CT: results in 44 cases. *Eur Radiol* 2009;19:619–25
- Psychogios MN, Buhk JH, Schramm P, et al. Feasibility of angiographic CT in peri-interventional diagnostic imaging: a comparative study with multidetector CT. *AJNR Am J Neuroradiol* 2010;31:1226–31
- Goyal M, Menon BK, van Zwam WH, et al. Endovascular thrombectomy after large-vessel ischaemic stroke: a meta-analysis of individual patient data from five randomised trials. *Lancet* 2016;387:1723–31
- Tan BY, Wan-Yee K, Paliwal P, et al. Good intracranial collaterals trump poor ASPECTS (Alberta Stroke Program Early CT Score) for intravenous thrombolysis in anterior circulation acute ischemic stroke. *Stroke* 2016;47:2292–8
- Lescher S, Reh C, Hoelter MC, et al. A novel reconstruction tool (syngo DynaCT Head Clear) in the post-processing of DynaCT images to reduce artefacts and improve image quality. *J Neurointerv Surg* Epub ahead of print: 19 Jan 2016. doi: 10.1136/neurintsurg-2015-012128
- Diekmann S, Siebert E, Juran R, et al. Dose exposure of patients undergoing comprehensive stroke imaging by multidetector-row CT: comparison of 320-detector row and 64-detector row CT scanners. *AJNR Am J Neuroradiol* 2010;31:1003–9
- Struffert T, Hauer M, Banckwitz R, et al. Effective dose to patient measurements in flat-detector and multislice computed tomography: a comparison of applications in neuroradiology. *Eur Radiol* 2014;24:1257–65
- Broderick JP, Palesch YY, Demchuk AM, et al. Endovascular therapy after intravenous t-PA versus t-PA alone for stroke. *N Engl J Med* 2013;368:893–903
- Kidwell CS, Jahan R, Gornbein J, et al. A trial of imaging selection and endovascular treatment for ischemic stroke. *N Engl J Med* 2013;368:914–23
- Ciccone A, Valvassori L. Endovascular treatment for acute ischemic stroke. *N Engl J Med* 2013;368:2433–4.
- Saver JL, Goyal M, van der Lugt A, et al. Time to treatment with endovascular thrombectomy and outcomes from ischemic stroke: a meta-analysis. *JAMA* 2016;316:1279–88
- Frei D, McGraw C, McCarthy K, et al. A standardized neurointerventional thrombectomy protocol leads to faster recanalization times. *J Neurointerv Surg* Epub ahead of print 3 Nov 2016. doi: 10.1136/neurintsurg-2016-012716
- Yang P, Niu K, Wu Y, et al. Time-resolved C-arm computed tomographic angiography derived from computed tomographic perfusion acquisition: new capability for one-stop-shop acute ischemic stroke treatment in the angi suite. *Stroke* 2015;46:3383–9
- Niu K, Yang P, Wu Y, et al. C-Arm conebeam CT perfusion imaging in the angiographic suite: a comparison with multidetector CT perfusion imaging. *AJNR Am J Neuroradiol* 2016;37:1303–9